METAL FRAMEWORK ARRANGEMENTS IN PENTANUCLEAR GOLD–RUTHENIUM CLUSTERS. CRYSTAL STRUCTURES OF [Au$_2$Ru$_3$(μ_3-S)(CO)$_8$(PPh$_3$)$_3$] AND [Au$_2$Ru$_3$(μ-H)(μ_3-COMe)(CO)$_9$(PPh$_3$)$_2$] *

LOUIS J. FARRUGIA, MARK J. FREEMAN, MICHAEL GREEN, A. GUY ORPEN, F. GORDON A. STONE, and IAN D. SALTER

Department of Inorganic Chemistry, University of Bristol, Bristol BS8 1TS (Great Britain)

(Received January 27th, 1983)

Summary

Reaction between the compounds [AuMe(PPh$_3$)] and [Ru$_3$(μ-H)$_2$(μ_3-S)(CO)$_9$] in toluene affords a mixture of products [AuRu$_3$(μ-H)(μ_3-S)(CO)$_8$(PPh$_3$)L] [Ru$_3$(μ-H)$_2$(μ_3-S)(CO)$_7$(PPh$_3$)L], and [Au$_2$Ru$_3$(μ_3-S)(CO)$_8$(PPh$_3$)$_2$L] (L = CO or PPh$_3$). The molecular structure of [Au$_2$Ru$_3$(μ_3-S)(CO)$_8$(PPh$_3$)$_3$] has been established by a single-crystal X-ray diffraction study. The Au$_2$Ru$_3$ metal atom core adopts a trigonal bipyramidal structure, with gold atoms occupying equatorial and apical sites. In contrast, in the species [Au$_2$Ru$_3$(μ-H)(μ_3-COMe)(CO)$_9$(PPh$_3$)$_2$], also studied by X-ray diffraction, the metal atoms have a distorted square pyramidal structure with a ruthenium atom at the apex. These structural studies allow interpretation of the dynamic behaviour of [Au$_2$Ru$_3$(μ_3-S)(CO)$_8$(PPh$_3$)$_3$], observed in solution by NMR measurements. It is proposed that facile Au–Ru bond rupture takes place to afford an intermediate with a square pyramidal Au$_2$Ru$_3$ core, as found in [Au$_2$Ru$_3$(μ-H)(μ_3-COMe)(CO)$_9$(PPh$_3$)$_2$].

Introduction

Several heteronuclear metal cluster compounds containing AuPPh$_3$ groups have recently been reported [1–6]. Generally the AuPPh$_3$ unit replaces a hydrido ligand, frequently adopting bonding modes reminiscent of this ligand in cluster chemistry, e.g. bridging metal–metal bonds or capping triangulated faces. It has become evident, however, that when more than one gold atom is present in a cluster there is a pronounced tendency towards formation of gold–gold bonds [2,3,5]. In exploring the chemistry of some pentanuclear digold–triruthenium complexes we have observed two ground state metal core geometries of which one is undergoing a polytopal rearrangement in solution on the NMR time scale.

Results and discussion

Reaction of the compound $[Ru_3(\mu\text{-}H)_2(\mu_3\text{-}S)(CO)_9]$ [7] in toluene at 60°C with two mole equivalents of $[AuMe(PPh_3)]$ affords a mixture of products (I–VI) partially separated by chromatography on alumina.

Compound I was characterised by microanalysis and spectroscopic properties (Experimental section). It is proposed that the $AuRu_3$ moiety in I has a similar geometry to that established for the metal core in $[AuRu_3(\mu\text{-}H)_2(\mu_3\text{-}COMe)(CO)_9(PPh_3)]$ by X-ray diffraction [3]. Moreover, the structure indicated for I is consistent with many other examples where the $AuPPh_3$ fragment occupies the position taken by the hydrido ligand in the precursor [1–4]. That I contains one of the hydrido ligands originally present in $[Ru_3(\mu\text{-}H)_2(\mu_3\text{-}S)(CO)_9]$ was established by the appearance of a doublet signal (J(PH) 2 Hz) at δ −19.78 in the ^{1}H NMR spectrum. The signal for the hydrido ligands in the related complex $[AuRu_3(\mu\text{-}H)_2(\mu_3\text{-}COMe)(CO)_9(PPh_3)]$ occurs at δ −18.62, also with J(PH) 2 Hz.
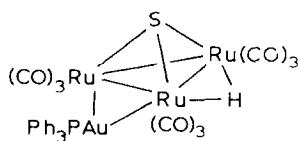
(I)
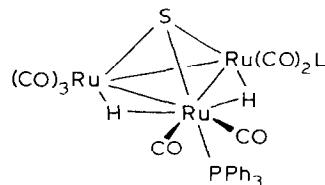
(II, L = CO;

IV, L = PPh₃)
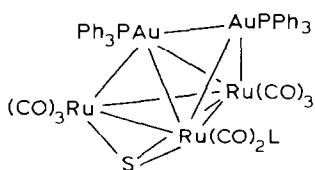
(V, L = CO;

VI, L = PPh₃)
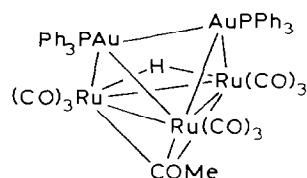
(VII)

Complex II, which does not contain a gold atom and is a PPh_3 derivative of the reactant $[Ru_3(\mu\text{-}H)_2(\mu_3\text{-}S)(CO)_9]$, was characterised by analytical and NMR data. The ^{1}H NMR spectrum shows a doublet resonance (J(PH) 10 Hz) for the hydrido ligands at δ −18.31. The ^{13}C-$\{^1$H$\}$ NMR spectrum at −60°C, having four peaks for the eight CO ligands, with one signal a doublet (J(PC) 9 Hz), is consistent with the structure shown for II.

Complex III could not be entirely separated from product IV by chromatography. The NMR data for the former, however, leave little doubt of its formulation as $[AuRu_3(\mu\text{-}H)(\mu_3\text{-}S)(CO)_8(PPh_3)_2]$; a derivative of I in which a CO ligand of one of the $Ru(CO)_3$ groups has been replaced by a PPh_3 group. The ^{31}P-$\{^1$H$\}$ NMR spectrum shows the expected doublet resonances (J(PP) 37 Hz) at δ 61.0 ($AuPPh_3$)

and 39.8 (RuPPh$_3$). The ^{1}H NMR spectrum of III has a resonance for the hydrido ligand at δ -19.13, which is a doublet of doublets due to coupling with the non-equivalent PPh$_3$ groups.

Compound IV, like II, is a PPh$_3$ derivative of [Ru$_3$(μ-H)$_2$(μ_3-S)(CO)$_9$]. The NMR data are in agreement with the structure shown. There are two resonances in the ^{31}P-$\{^1$H$\}$ spectrum, and the ^{13}C-$\{^1$H$\}$ spectrum, measured at $-60°$C, shows seven peaks for the non-equivalent CO ligands. However, alternative structures to that depicted, with the PPh$_3$ groups arranged so that there is no plane of symmetry in the molecule, cannot be ruled out. In order to confirm the formulations of compounds II and IV they were independently prepared by reacting PPh$_3$ with [Ru$_3$(μ-H)$_2$(μ_3-S)(CO)$_9$].

Study of the ^{31}P-$\{^1$H$\}$ and ^{13}C-$\{^1$H$\}$ NMR spectra of V and VI implied that these species were undergoing dynamic behaviour in solution. Moreover, it was evident from analytical and other data that VI had a formulation similar to V with a CO group in the latter replaced by PPh$_3$. In order to establish the molecular structures in the solid state, an X-ray crystallographic study was carried out on VI. Discussion of the NMR data is deferred until the X-ray diffraction results have been described.

Selected bond distances and angles for VI as its hemi-dichloromethane solvate are given in Table 1 and the molecular structure is illustrated in Fig. 1. The metal core atoms adopt a trigonal bipyramidal arrangement, as expected on the basis of the six skeletal electron pairs available [8]. A salient point of interest in the structure is that one gold atom occupies an apical position and the other an equatorial site in the
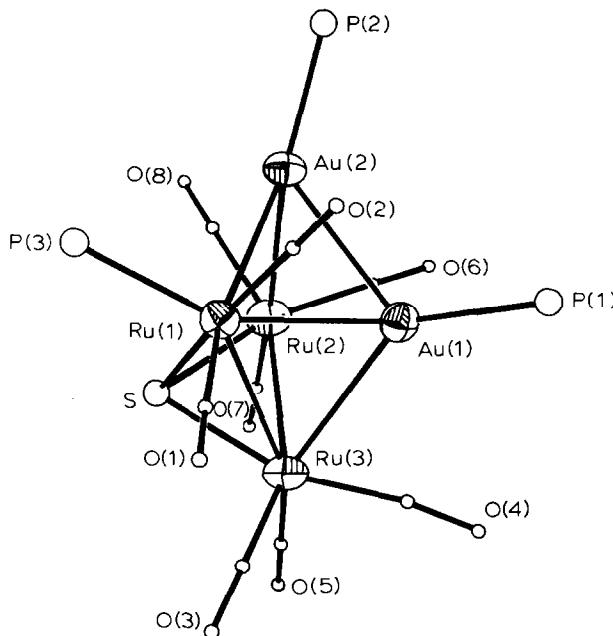
Fig. 1. Molecular structure of [Au$_2$Ru$_3$(μ_3-S)(CO)$_8$(PPh$_3$)$_3$] (VI); phenyl groups have been omitted for clarity and non-metal atoms drawn as circles of arbitrary radius. Metal atoms are drawn to enclose 50% probability density. Only oxygen atoms of CO ligands have been labelled for clarity of presentation; carbon atoms of these groups are numbered as are their respective oxygens.

TABLE 1

SELECTED BOND DISTANCES (Å) AND ANGLES (°) FOR COMPOUND $[Au_2Ru_3(\mu_3\text{-}S)(CO)_8(PPh_3)_3]\cdot\frac{1}{2}CH_2Cl_2$ (VI)

Au(1)–Au(2)	2.915(2)	Au(1)–Ru(1)	2.784(2)
Au(1)–Ru(2)	2.861(2)	Au(1)–Ru(3)	2.897(2)
Au(1)–P(1)	2.305(3)	Au(2)–Ru(1)	2.796(2)
Au(2)–Ru(2)	2.807(2)	Au(2)–P(2)	2.310(3)
Ru(1)–Ru(2)	3.034(2)	Ru(1)–Ru(3)	2.883(2)
Ru(1)–P(3)	2.354(3)	Ru(1)–S(1)	2.354(3)
Ru(1)–C(1)	1.849(12)	Ru(1)–C(2)	1.883(10)
Ru(2)–Ru(3)	2.833(2)	Ru(2)–S(1)	2.366(3)
Ru(2)–C(6)	1.893(11)	Ru(2)–C(7)	1.882(11)
Ru(2)–C(8)	1.903(13)	Ru(3)–S(1)	2.349(3)
Ru(3)–C(3)	1.880(16)	Ru(3)–C(4)	1.900(11)
Ru(3)–C(5)	1.897(12)	P(1)–C(111)	1.815(10)
P(1)–C(121)	1.809(9)	P(1)–C(131)	1.845(11)
P(2)–C(211)	1.806(10)	P(2)–C(221)	1.833(11)
P(2)–C(231)	1.812(10)	P(3)–C(311)	1.827(11)
P(3)–C(321)	1.832(9)	P(3)–C(331)	1.842(11)
O(1)–C(1)	1.162(16)	O(2)–C(2)	1.163(12)
O(3)–C(3)	1.144(21)	O(4)–C(4)	1.148(14)
O(5)–C(5)	1.130(15)	O(6)–C(6)	1.158(15)
O(7)–C(7)	1.130(14)	O(8)–C(8)	1.133(17)
Au(2)–Au(1)–Ru(1)	58.7(1)	Au(2)–Au(1)–Ru(2)	58.1(1)
Ru(1)–Au(1)–Ru(2)	65.0(1)	Au(2)–Au(1)–Ru(3)	105.2(1)
Ru(1)–Au(1)–Ru(3)	61.0(1)	Ru(2)–Au(1)–Ru(3)	58.9(1)
Au(2)–Au(1)–P(1)	119.5(1)	Ru(1)–Au(1)–P(1)	138.1(1)
Ru(2)–Au(1)–P(1)	154.8(1)	Ru(3)–Au(1)–P(1)	134.7(1)
Au(1)–Au(2)–Ru(1)	58.3(1)	Au(1)–Au(2)–Ru(2)	60.0(1)
Ru(1)–Au(2)–Ru(2)	65.6(1)	Au(1)–Au(2)–P(2)	128.8(1)
Ru(1)–Au(2)–P(2)	153.1(1)	Ru(2)–Au(2)–P(2)	141.3(1)
Au(1)–Ru(1)–Au(2)	63.0(1)	Au(1)–Ru(1)–Ru(2)	58.7(1)
Au(2)–Ru(1)–Ru(2)	57.4(1)	Au(1)–Ru(1)–Ru(3)	61.5(1)
Au(2)–Ru(1)–Ru(3)	108.7(1)	Ru(2)–Ru(1)–Ru(3)	57.2(1)
Au(1)–Ru(1)–P(3)	152.3(1)	Au(2)–Ru(1)–P(3)	89.6(1)
Ru(2)–Ru(1)–P(3)	111.1(1)	Ru(3)–Ru(1)–P(3)	138.3(1)
Au(1)–Ru(1)–S(1)	99.7(1)	Au(2)–Ru(1)–S(1)	100.4(1)
Ru(2)–Ru(1)–S(1)	50.2(1)	Ru(3)–Ru(1)–S(1)	52.1(1)
P(3)–Ru(1)–S(1)	88.6(1)	Au(1)–Ru(1)–C(1)	107.9(3)
Au(2)–Ru(1)–C(1)	156.1(3)	Ru(2)–Ru(1)–C(1)	139.3(3)
Ru(3)–Ru(1)–C(1)	82.4(3)	P(3)–Ru(1)–C(1)	95.7(3)
S(1)–Ru(1)–C(1)	103.0(3)	Au(1)–Ru(1)–C(2)	71.2(3)
Au(2)–Ru(1)–C(2)	71.2(4)	Ru(2)–Ru(1)–C(2)	119.5(3)
Ru(3)–Ru(1)–C(2)	123.7(3)	P(3)–Ru(1)–C(2)	97.3(3)
S(1)–Ru(1)–C(2)	169.6(3)	C(1)–Ru(1)–C(2)	85.0(5)
Au(1)–Ru(2)–Au(2)	61.9(1)	Au(1)–Ru(2)–Ru(1)	56.3(1)
Au(2)–Ru(2)–Ru(1)	57.0(1)	Au(1)–Ru(2)–Ru(3)	61.2(1)
Au(2)–Ru(2)–Ru(3)	109.8(1)	Ru(1)–Ru(2)–Ru(3)	58.8(1)
Au(1)–Ru(2)–S(1)	97.3(1)	Au(2)–Ru(2)–S(1)	99.8(1)
Ru(1)–Ru(2)–S(1)	49.8(1)	Ru(3)–Ru(2)–S(1)	52.8(1)
Au(1)–Ru(2)–C(6)	69.7(4)	Au(2)–Ru(2)–C(6)	83.4(3)
Ru(1)–Ru(2)–C(6)	122.9(3)	Ru(3)–Ru(2)–C(6)	110.7(4)
S(1)–Ru(2)–C(6)	163.4(4)	Au(1)–Ru(2)–C(7)	129.3(4)
Au(2)–Ru(2)–C(7)	164.5(4)	Ru(1)–Ru(2)–C(7)	136.6(4)
Ru(3)–Ru(2)–C(7)	85.7(4)	S(1)–Ru(2)–C(7)	89.9(4)

TABLE 1 (continued)

C(6)–Ru(2)–C(7)	90.8(5)	Au(1)–Ru(2)–C(8)	129.6(3)
Au(2)–Ru(2)–C(8)	69.5(3)	Ru(1)–Ru(2)–C(8)	106.8(3)
Ru(3)–Ru(2)–C(8)	156.1(4)	S(1)–Ru(2)–C(8)	103.3(4)
C(6)–Ru(2)–C(8)	93.1(5)	C(7)–Ru(2)–C(8)	96.5(5)
Au(1)–Ru(3)–Ru(1)	57.6(1)	Au(1)–Ru(3)–Ru(2)	59.9(1)
Ru(1)–Ru(3)–Ru(2)	64.1(1)	Au(1)–Ru(3)–S(1)	96.7(1)
Ru(1)–Ru(3)–S(1)	52.3(1)	Ru(2)–Ru(3)–S(1)	53.3(1)
Au(1)–Ru(3)–C(3)	127.6(4)	Ru(1)–Ru(3)–C(3)	96.6(4)
Ru(2)–Ru(3)–C(3)	152.7(4)	S(1)–Ru(3)–C(3)	99.8(4)
Au(1)–Ru(3)–C(4)	65.3(3)	Ru(1)–Ru(3)–C(4)	114.4(3)
Ru(2)–Ru(3)–C(4)	111.5(4)	S(1)–Ru(3)–C(4)	161.8(3)
C(3)–Ru(3)–C(4)	93.7(5)	Au(1)–Ru(3)–C(5)	133.0(4)
Ru(1)–Ru(3)–C(5)	152.1(4)	Ru(2)–Ru(3)–C(5)	97.4(5)
S(1)–Ru(3)–C(5)	100.2(4)	C(3)–Ru(3)–C(5)	92.1(6)
C(4)–Ru(3)–C(5)	91.4(5)	Au(1)–P(1)–C(111)	119.8(3)
Au(1)–P(1)–C(121)	113.7(3)	C(111)–P(1)–C(121)	103.4(4)
Au(1)–P(1)–C(131)	110.1(3)	C(111)–P(1)–C(131)	102.5(5)
C(121)–P(1)–C(131)	105.9(5)	Au(2)–P(2)–C(211)	112.7(3)
Au(2)–P(2)–C(221)	112.6(3)	C(211)–P(2)–C(221)	105.1(5)
Au(2)–P(2)–C(231)	116.1(4)	C(211)–P(2)–C(231)	105.2(4)
C(221)–P(2)–C(231)	104.1(4)	Ru(1)–P(3)–C(311)	118.6(3)
Ru(1)–P(3)–C(321)	116.3(3)	C(311)–P(3)–C(321)	105.0(5)
Ru(1)–P(3)–C(331)	112.3(3)	C(311)–P(3)–C(331)	101.7(5)
C(231)–P(3)–C(331)	100.3(4)	Ru(1)–S(1)–Ru(2)	80.0(1)
Ru(1)–S(1)–Ru(3)	75.6(1)	Ru(2)–S(1)–Ru(3)	73.9(1)
Ru(1)–C(1)–O(1)	172.6(9)	Ru(1)–C(2)–O(2)	172.7(10)
Ru(3)–C(3)–O(3)	173.6(12)	Ru(3)–C(4)–O(4)	171.1(9)
Ru(3)–C(5)–O(5)	178.5(14)	Ru(2)–C(6)–O(6)	171.4(10)
Ru(2)–C(7)–O(7)	179.3(12)	Ru(2)–C(8)–O(8)	169.7(10)

trigonal bipyramid. The Ru_3 unit is preserved intact and forms a triangular face of the cluster, with the sulphur atom capping that face, and formally acting as a four electron donor, as in the precursor $[Ru_3(\mu\text{-H})_2(\mu_3\text{-S})(CO)_9]$ [7]. The phosphine substituted ruthenium atom occupies one of the equatorial sites. The cluster geometry may be considered to be derived from one in which two $AuPPh_3$ moieties bridge two edges of the Ru_3 triangle, as the hydrido ligands do in $[Ru_3(\mu\text{-H})_2(\mu_3\text{-S})(CO)_9]$. However, in VI the molecule has a *closo* structure due to formation of Au–Au and Au–Ru bonds.

The Ru–Ru separations show appreciable differences, varying between 2.833(2) and 3.034(2) Å, the longest being in the equatorial plane of the trigonal bipyramid. Likewise, the Au–Ru distances vary between 2.784(2) and 2.897(2) Å. The Au–Au separation (2.915(2) Å) is in the range previously observed (2.784(1) to 3.010(1) Å) for such distances in heteronuclear metal clusters [2,3,5], and is only slightly longer than that (2.884 Å) in gold metal [9]. In general, in homonuclear clusters containing $AuPPh_3$ groups the shorter and stronger metal–metal interactions are those most nearly *trans* to the PR_3 ligands [10]. The metal–phosphorus distances themselves are typical of those found in metal cluster complexes.

The CO ligands in VI are all terminally bound and the M–C–O groups essentially linear, those deviating most markedly from linearity are involved in weak interactions with gold atoms; this last is a common feature in heteronuclear metal clusters

containing CO ligands in proximity to Au atoms with relatively sparsely populated coordination spheres. The μ_3-S ligand shows very small deviations from symmetric capping of the Ru_3 triangle, the longest Ru–S distances being to the two ruthenium atoms in the equatorial plane Ru(1)–S, 2.354(3); Ru(2)–S, 2.366(3); Ru(3)–S, 2.349(3) Å.

Having established the trigonal bipyramidal arrangement of the Au_2Ru_3 core in VI we were concerned to establish the arrangement of the metal atoms in $[Au_2Ru_3(\mu\text{-H})(\mu_3\text{-COMe})(CO)_9(PPh_3)_2]$ (VII), one of several products of the reaction of $[Ru_3(\mu\text{-H})_3(\mu_3\text{-COMe})(CO)_9]$ with $[AuMe(PPh_3)]$ [3]. The results of this study are given in Table 2, and the molecular structure is shown in Fig. 2.

It is immediately apparent that the Au_2Ru_3 core in VII adopts an asymmetric square pyramidal structure with Ru(3) at the apex. The metal–metal separations in the basal plane vary from 3.176(1) (Au(1)–Au(2)) to 2.735(1) Å (Au(1)–Ru(2)), and there is similar asymmetry in the apical-basal distances of 2.899(2) (Ru(2)–Ru(3)) to 2.702(1) Å (Au(2)–Ru(3)). This is partly due to differences in the atomic radii of gold and ruthenium. This can be seen in the Ru–Ru separations in VII which are from 2.860(1) to 2.899(2) Å whilst the Au–Ru distances, which range from 2.796(1) to 2.702(1) Å, are approximately 0.1 Å smaller. The latter range is similar to that found in related compounds where the gold atoms are bonded to only two ruthenium atoms [3,6,11]. The Au(1)–Au(2) separation in VII (3.176(1) Å) is distinctly longer than that in VI (2.915(2) Å) and is at the top end of the range for such separations, mentioned above.

The capping carbyne ligand in VII spans the Ru_3 face somewhat asymmetrically, with Ru–C(10) distances 2.064(13), 2.080(10), and 2.103(13) Å. The bridging μ_3-CMe
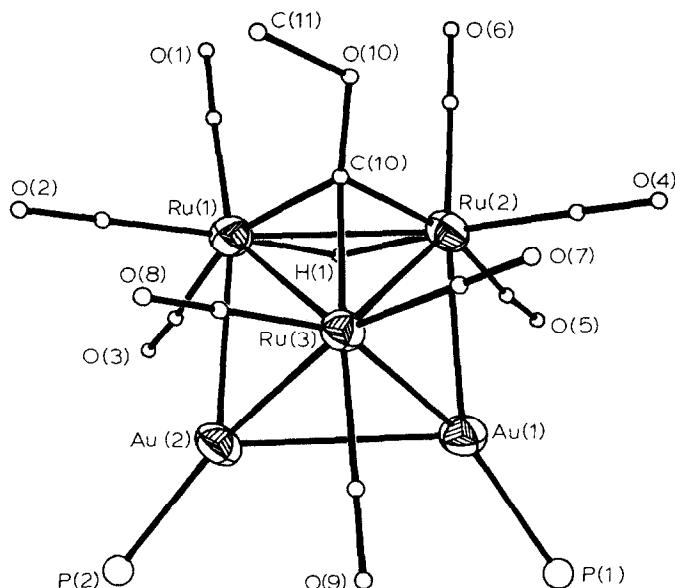

Fig. 2. Molecular structure of $[Au_2Ru_3(\mu\text{-H})(\mu_3\text{-COMe})(CO)_9(PPh_3)_2]$ (VII). Phenyl groups and methyl hydrogens have been omitted for clarity and non-metal atoms drawn as circles of arbitrary radius. Metal atoms are drawn to enclose 50% probability density.

TABLE 2

SELECTED BOND DISTANCES (Å) AND ANGLES (°) FOR COMPOUND $[Au_2Ru_3(\mu\text{-H})(\mu_3\text{-COMe})(CO)_9(PPh_3)_2]$ (VII)

Au(1)–Au(2)	3.176(1)	Au(1)–Ru(2)	2.735(1)
Au(1)–Ru(3)	2.749(1)	Au(1)–P(1)	2.316(4)
Au(1)–C(9)	2.664(13)	Au(2)–Ru(1)	2.796(1)
Au(2)–Ru(3)	2.702(1)	Au(2)–P(2)	2.316(4)
Au(2)–C(3)	2.666(12)	Ru(1)–Ru(2)	2.860(1)
Ru(1)–Ru(3)	2.879(1)	Ru(1)–C(1)	1.881(14)
Ru(1)–C(2)	1.884(17)	Ru(1)–C(3)	1.968(13)
Ru(1)–C(10)	2.080(10)	Ru(2)–Ru(3)	2.899(2)
Ru(2)–C(4)	1.941(14)	Ru(2)–C(5)	1.963(14)
Ru(2)–C(6)	1.913(17)	Ru(2)–C(10)	2.064(13)
Ru(3)–C(7)	1.911(11)	Ru(3)–C(8)	1.885(15)
Ru(3)–C(9)	1.956(14)	Ru(3)–C(10)	2.103(13)
P(1)–C(111)	1.818(9)	P(1)–C(121)	1.820(9)
P(1)–C(131)	1.828(10)	P(2)–C(211)	1.810(10)
P(2)–C(221)	1.812(11)	P(2)–C(231)	1.783(12)
O(1)–C(1)	1.138(19)	O(2)–C(2)	1.139(23)
O(3)–C(3)	1.162(15)	O(4)–C(4)	1.119(17)
O(5)–C(5)	1.126(19)	O(6)–C(6)	1.133(22)
O(7)–C(7)	1.132(13)	O(8)–C(8)	1.142(19)
O(9)–C(9)	1.147(17)	O(10)–C(10)	1.371(15)
O(10)–C(11)	1.420(23)		
Au(2)–Au(1)–Ru(2)	88.7(1)	Au(2)–Au(1)–Ru(3)	53.7(1)
Ru(2)–Au(1)–Ru(3)	63.8(1)	Au(2)–Au(1)–P(1)	122.7(1)
Ru(2)–Au(1)–P(1)	143.3(1)	Ru(3)–Au(1)–P(1)	148.9(1)
Au(2)–Au(1)–C(9)	54.1(2)	Ru(2)–Au(1)–C(9)	106.1(3)
Ru(3)–Au(1)–C(9)	42.3(3)	P(1)–Au(1)–C(9)	107.9(3)
Au(1)–Au(2)–Ru(1)	84.7(1)	Au(1)–Au(2)–Ru(3)	55.1(1)
Ru(1)–Au(2)–Ru(3)	63.1(1)	Au(1)–Au(2)–P(2)	126.7(1)
Ru(1)–Au(2)–P(2)	134.2(1)	Ru(3)–Au(2)–P(2)	160.3(1)
Au(1)–Au(2)–C(3)	101.8(3)	Ru(1)–Au(2)–C(3)	42.1(3)
Ru(3)–Au(2)–C(3)	104.4(3)	P(2)–Au(2)–C(3)	94.5(3)
Au(2)–Ru(1)–Ru(2)	94.2(1)	Au(2)–Ru(1)–Ru(3)	56.8(1)
Ru(2)–Ru(1)–Ru(3)	60.7(1)	Au(2)–Ru(1)–C(1)	161.5(4)
Ru(2)–Ru(1)–C(1)	97.0(5)	Ru(3)–Ru(1)–C(1)	141.7(4)
Au(2)–Ru(1)–C(2)	86.4(5)	Ru(2)–Ru(1)–C(2)	147.2(4)
Ru(3)–Ru(1)–C(2)	93.4(3)	C(1)–Ru(1)–C(2)	92.1(7)
Au(2)–Ru(1)–C(3)	65.4(4)	Ru(2)–Ru(1)–C(3)	116.0(4)
Ru(3)–Ru(1)–C(3)	121.0(4)	C(1)–Ru(1)–C(3)	96.4(5)
C(2)–Ru(1)–C(3)	94.1(6)	Au(2)–Ru(1)–C(10)	103.4(3)
Ru(2)–Ru(1)–C(10)	46.1(4)	Ru(3)–Ru(1)–C(10)	46.8(4)
C(1)–Ru(1)–C(10)	95.0(5)	C(2)–Ru(1)–C(10)	101.8(5)
C(3)–Ru(1)–C(10)	160.1(5)	Au(1)–Ru(2)–Ru(1)	92.3(1)
Au(1)–Ru(2)–Ru(3)	58.3(1)	Ru(1)–Ru(2)–Ru(3)	60.0(1)
Au(1)–Ru(2)–C(4)	88.0(5)	Ru(1)–Ru(2)–C(4)	144.8(5)
Ru(3)–Ru(2)–C(4)	91.1(5)	Au(1)–Ru(2)–C(5)	70.3(5)
Ru(1)–Ru(2)–C(5)	117.6(4)	Ru(3)–Ru(2)–C(5)	127.9(5)
C(4)–Ru(2)–C(5)	95.6(5)	Au(1)–Ru(2)–C(6)	166.8(5)
Ru(1)–Ru(2)–C(6)	94.0(5)	Ru(3)–Ru(2)–C(6)	134.6(5)
C(4)–Ru(2)–C(6)	93.5(7)	C(5)–Ru(2)–C(6)	96.5(7)
Au(1)–Ru(2)–C(10)	104.4(4)	Ru(1)–Ru(2)–C(10)	46.6(3)
Ru(3)–Ru(2)–C(10)	46.5(4)	C(4)–Ru(2)–C(10)	99.4(6)
C(5)–Ru(2)–C(10)	164.0(5)	C(6)–Ru(2)–C(10)	88.3(6)

TABLE 2 (continued)

Au(1)–Ru(3)–Au(2)	71.3(1)	Au(1)–Ru(3)–Ru(1)	91.6(1)
Au(2)–Ru(3)–Ru(1)	60.0(1)	Au(1)–Ru(3)–Ru(2)	57.9(1)
Au(2)–Ru(3)–Ru(2)	95.4(1)	Ru(1)–Ru(3)–Ru(2)	59.3(1)
Au(1)–Ru(3)–C(7)	99.4(4)	Au(2)–Ru(3)–C(7)	162.5(4)
Ru(1)–Ru(3)–C(7)	136.4(4)	Ru(2)–Ru(3)–C(7)	91.6(4)
Au(1)–Ru(3)–C(8)	156.0(5)	Au(2)–Ru(3)–C(8)	90.3(4)
Ru(1)–Ru(3)–C(8)	92.2(3)	Ru(2)–Ru(3)–C(8)	141.8(4)
C(7)–Ru(3)–C(8)	94.1(5)	Au(1)–Ru(3)–C(9)	66.5(4)
Au(2)–Ru(3)–C(9)	68.5(3)	Ru(1)–Ru(3)–C(9)	128.3(3)
Ru(2)–Ru(3)–C(9)	124.3(4)	C(7)–Ru(3)–C(9)	94.3(5)
C(8)–Ru(3)–C(9)	92.9(6)	Au(1)–Ru(3)–C(10)	102.8(4)
Au(2)–Ru(3)–C(10)	106.0(3)	Ru(1)–Ru(3)–C(10)	46.2(3)
Ru(2)–Ru(3)–C(10)	45.4(4)	C(7)–Ru(3)–C(10)	90.3(5)
C(8)–Ru(3)–C(10)	96.8(6)	C(9)–Ru(3)–C(10)	168.9(5)
Au(1)–P(1)–C(111)	108.8(4)	Au(1)–P(1)–C(121)	114.9(4)
Au(1)–P(1)–C(131)	118.2(3)	Au(2)–P(2)–C(211)	116.8(3)
Au(2)–P(2)–C(221)	115.0(4)	Au(2)–P(2)–C(231)	110.7(4)
C(10)–O(10)–C(11)	117.8(12)	Ru(1)–C(1)–O(1)	177.5(14)
Ru(1)–C(2)–O(2)	179.8(15)	Au(2)–C(3)–Ru(1)	72.5(3)
Au(2)–C(3)–O(3)	117.4(11)	Ru(1)–C(3)–O(3)	169.4(14)
Ru(2)–C(4)–O(4)	177.3(15)	Ru(2)–C(5)–O(5)	172.5(14)
Ru(2)–C(6)–O(6)	179.0(13)	Ru(3)–C(7)–O(7)	177.2(13)
Ru(3)–C(8)–O(8)	175.4(9)	Au(1)–C(9)–Ru(3)	71.1(4)
Au(1)–C(9)–O(9)	119.6(10)	Ru(3)–C(9)–O(9)	166.6(9)
Ru(1)–C(10)–Ru(2)	87.3(4)	Ru(1)–C(10)–Ru(3)	87.0(5)
Ru(2)–C(10)–Ru(3)	88.1(5)	Ru(1)–C(10)–O(10)	131.1(8)
Ru(2)–C(10)–O(10)	121.3(10)	Ru(3)–C(10)–O(10)	128.5(7)

ligand in $[Ru_3(\mu\text{-}H)_3(\mu_3\text{-}CMe)(CO)_9]$ is more symmetrically bound with μ_3-C–Ru distances in the range 2.078(12)–2.086(10) Å [12]. In species more closely related to VII, asymmetry of the μ_3-COMe ligand was also observed [3].

The presence of the hydrido ligand in VII was not established by the X-ray diffraction data. However, calculations based on potential-energy minima [13] accord with H bridging the Ru(1)–Ru(2) edge (Fig. 2). Moreover, the ^{1}H NMR spectrum shows the characteristic resonance of this group at δ − 19.00, a triplet with J(PH) 2 Hz [3]. In accord with this data, we assume the hydride bridged the Ru(1)–Ru(2) bond, as expected since AuPPh$_3$ groups bridge the other edges of the Ru$_3$ triangle.

Like VI, compound VII has 72 cluster valence electrons but unlike the former the nido-structure of the latter violates skeletal electron pair theory [8,14,15]. Having established the structures of these two species it is possible to discuss the NMR data.

As is typical of metal cluster compounds, the CO ligands in V and VI are undergoing site exchange in solution. The ^{13}C-{^{1}H} NMR spectrum of V at − 70°C shows only one CO resonance. The spectrum of VI at room temperature shows two CO signals with relative intensity 2/6 corresponding to the Ru(CO)$_2$PPh$_3$ and Ru(CO)$_3$ groups. Poor solubility of VI prevented ^{13}C-{^{1}H} measurements at low temperature. However, clearly the ground state structure had not been attained at room temperature since eight resonances would be expected based on the structure in the crystal (Fig. 1). The ^{31}P-{^{1}H} NMR spectra of V and VI show only one resonance for the AuPPh$_3$ groups down to − 90°C. The spectrum of VI also shows a

resonance for the $RuPPh_3$ group, but this appears as a triplet (J(PP) 18 Hz) reflecting, on the NMR time-scale, coupling with two apparently chemically equivalent $AuPPh_3$ groups. Moreover, no change occurred in the spectrum upon addition of PPh_3, other than the appearance of a signal due to the latter. The coupling between the $AuPPh_3$ and $RuPPh_3$ groups (18 Hz) remains unaltered. Evidently PPh_3 dissociation from VI was not responsible for the time averaged resonance observed at $-90°C$. The ^{31}P-{^1H} NMR data are thus at variance with the results of the X-ray diffraction study on VI which revealed in the solid state gold atoms in both an apical and an equatorial site in the trigonal bipyramid.

Evidently for V and VI, there is a rearrangement of the metal atom core in solution with concomitant site exchange of CO groups. To explain the results we postulate that the metal atoms undergo a Berry-type mechanism involving a square pyramidal intermediate (Fig. 3). That such a structure is possible for a Au_2Ru_3 core is established by the X-ray diffraction results for VII. Clearly the scission of Au–Ru bonds is involved in the scheme shown in Fig. 3. Evidently rupture of a Au–Ru bond requires relatively little energy. Theoretical and experimental studies on homonuclear clusters $[Au_9(PR_3)_8]^{3+}$ indicate that the strengths of Au–Au bonds essentially perpendicular to the Au–P vectors are weak [10,16]. The present study suggests that this is also true for heteronuclear metal–metal bonds involving gold. The rearrangement of VI in solution cannot be a full Berry *pseudo*-rotation since the three ruthenium atoms are constrained to remain bonded to one another by the μ_3-S ligand.

Apparently in VII the barrier to forming the trigonal bipyramidal structure is the presence of the hydrido ligand which blocks the site to which a gold atom could collapse to form a Au–Ru bond. The ruthenium atoms Ru(1) and Ru(2) in VII (Fig. 2) are ligated by five atoms, not counting the three metal–metal bonds. In VI (Fig. 1) the ruthenium atoms, ignoring the metal–metal contacts, are bonded to just four groups.
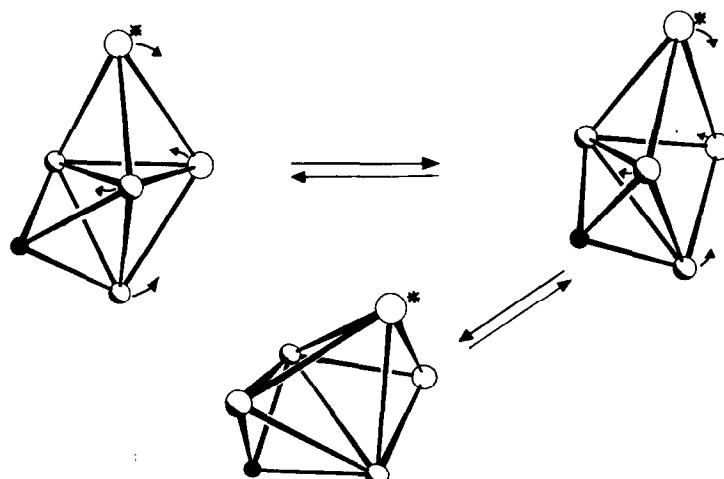

Fig. 3. Interconversion of trigonal bipyramidal and square pyramidal forms of V or VI leading to exchange between gold sites: a restricted Berry *pseudo*-rotation. Filled circle is S, shaded circles Ru, and circles are Au atoms.

Experimental

The compound [Ru$_3$(μ-H)$_2$(μ_3-S)(CO)$_9$] was prepared as described elsewhere [7]. Infrared spectra were recorded with a Nicolet FT MX-1 spectrophotometer, in cyclohexane solutions unless otherwise stated. NMR measurements were made with a JEOL FX 90Q instrument, and chemical shifts for ^{31}P-{^{1}H} spectra are positive to high frequency of 85% H$_3$PO$_4$ (external), and for ^{13}C-{^{1}H} are positive to high frequency of SiMe$_4$. Spectra were recorded in CDCl$_3$ (^{1}H and ^{31}P-{^{1}H}) and CD$_2$Cl$_2$/CH$_2$Cl$_2$ (^{13}C-{^{1}H}), unless stated to the contrary. For the ^{13}C-{^{1}H} measurements, Cr(acac)$_3$ was added. Solvents were freshly distilled from the usual drying agents immediately before use, and all reactions and manipulations were carried out under nitrogen using Schlenk tube techniques. Light petroleum refers to that fraction b.p. 40–60°C. Yields of new compounds are expressed in terms of the ruthenium complex taken for reaction.

Reaction of [Ru$_3$(μ-H)$_2$(μ_3-S)(CO)$_9$] with [AuMe(PPh$_3$)]

A mixture of [Ru$_3$(μ-H)$_2$(μ_3-S)(CO)$_9$] (0.40 g, 0.68 mmol) and [AuMe(PPh$_3$)] (0.65 g, 1.37 mmol) in toluene (80 cm^3) was placed in a Schlenk tube fitted with a Young's high pressure stopcock. After freezing the reactants with liquid nitrogen, the reaction vessel was evacuated, sealed, and heated at 60°C overnight. All volatile material was removed by pumping in vacuo and the residue was dissolved in a dichloromethane/light petroleum mixture (1/5) and chromatographed on an alumina column (20 × 2 cm). The column was eluted with dichloromethane/light petroleum mixtures, initially in the proportion 1/5, subsequently changing to 1/3, and finally to 1/1 to elute the last band. Four bands were obtained from the column, and after evaporation of solvent gave:

(a) Orange crystals of [AuRu$_3$(μ-H)(μ_3-S)(CO)$_9$(PPh$_3$)] (I) (0.03 g, 4%) and yellow crystals of [Ru$_3$(μ-H)$_2$(μ_3-S)(CO)$_8$(PPh$_3$)] (II) (0.04 g, 7%), crystallised from light petroleum. The two species were separeted by hand picking of crystals under a microscope.

(b) Yellow microcrystals of [Ru$_3$(μ-H)$_2$(μ_3-S)(CO)$_7$(PPh$_3$)$_2$] (IV) (0.12 g, 17%), obtained pure by crystallisation from diethyl ether/light petroleum. The first one-third of the yellow band containing IV eluting from the column also contained [AuRu$_3$(μ-H)(μ_3-S)(CO)$_8$(PPh$_3$)$_2$] (III), and it was not possible to separate the two species. Consequently, the latter was identified spectroscopically (see below) in the mixture.

(c) Red crystals of [Au$_2$Ru$_3$(μ_3-S)(CO)$_9$(PPh$_3$)$_2$] (V) (0.27 g, 26%), recrystallised from dichloromethane/light petroleum.

(d) Brown crystals of [Au$_2$Ru$_3$(μ_3-S)(CO)$_8$(PPh$_3$)$_2$] (VI) (0.21 g, 18%) crystallised from dichloromethane/light petroleum.

The products were identified by microanalysis, and by IR and NMR data:

(i) Compound I, m.p. 155–158°C decomp., (Found: C, 31.5; H, 1.5. C$_{27}$H$_{16}$AuO$_9$PRu$_3$S calcd.: C, 30.9; H, 1.5%). IR, ν(CO) 2084m, 2062vs, 2036vs, 1999s, 1992s, 1978w, 1956w cm^{-1}. NMR, ^{1}H, δ 7.47 (m br, 15H, Ph), −19.78 (d, 1H, RuH, J(PH) 2 Hz); ^{31}P-{^{1}H}, δ 62.8 ppm (s, AuPPh$_3$).

(ii) Compound II, m.p. 169–173°C decomp., (Found: C, 37.6; H, 2.1. C$_{26}$H$_{17}$O$_8$PRu$_3$S calcd.: C, 37.9; H, 2.1%). IR, ν(CO) 2081m, 2053s, 2048vs, 2006vs, 1996m, 1988w, 1980w, 1957vw cm^{-1}. NMR, ^{1}H, δ 7.45 (m br, 15H, Ph), −18.31 (d,

2H, RuH, J(PH) 10 Hz); ^{31}P-{^{1}H}, δ 38.3 ppm (s, RuPPh$_3$); ^{13}C-{^{1}H} ($-60°$C), δ 198.1 (2 × CO), 194.8 (2 × CO), 188.8 (d, 2 × CO, J(PC) 9 Hz), 188.1 (2 × CO), 134.2 (Ph), 133.4 (d, C^2(Ph), J(PC) 12 Hz), 131.2 (Ph), 129.2 ppm (d, C^3(Ph), J(PC) 10 Hz).

(iii) The NMR data for III were obtained by subtracting the peaks due to IV from a spectrum of a mixture of the two species. ^{1}H, δ -19.13 (d of d, RuH, J(PH) 8 and 2 Hz); ^{31}P-{^{1}H}, δ 61.0 (d, AuPPh$_3$, J(PP) 37 Hz), 39.8 ppm (d, RuPPh$_3$, J(PP) 37 Hz).

(iv) Compound IV, m.p. 196–200°C decomp., (Found: C, 49.0; H, 2.9. C$_{43}$H$_{32}$O$_7$P$_2$Ru$_3$S calcd.: C, 48.8; H, 3.0%). IR, ν(CO) 2060s, 2047vs, 2004vs, 1989s, 1972m, 1844w cm^{-1}. NMR, ^{1}H, δ 7.30 (m br, 30H, Ph), -17.67 (d, 2H, RuH, J(PH) 10 Hz); ^{31}P-{^{1}H}, δ 36.8, 36.0 ppm (RuPPh$_3$); ^{13}C-{^{1}H} ($-60°$C), δ 203.7 (d, CO, J(PC) 7 Hz), 200.7 (CO), 199.1 (d, CO, J(PC) 7 Hz), 196.5 (CO), 189.3 (d, CO, J(PC) 9 Hz), 188.8 (d, CO, J(PC) 7 Hz), 188.5 (CO), 136.0 and 134.5 (d, C^1(Ph), J(PC) 41 and 48 Hz), 133.6 and 133.5 (d, C^2(Ph), J(PC) 12 Hz), 130.9 and 130.2 (C^4(Ph)), 129.0 and 128.5 ppm (d, C^3(Ph), J(PC) 10 Hz).

(v) Compound V, m.p. 190–193°C decomp., (Found: C, 35.5; H, 2.2. C$_{45}$H$_{30}$Au$_2$O$_9$P$_2$Ru$_3$S · $\frac{1}{2}$CH$_2$Cl$_2$ calcd.: C, 35.3; H, 2.0%). IR, ν(CO) in CH$_2$Cl$_2$, 2055m, 2027vs, 2017vs, 1962s(br) cm^{-1}. NMR, ^{1}H, δ 7.33 (m br, Ph), ^{31}P-{^{1}H} (CD$_2$Cl$_2$/CH$_2$Cl$_2$, at $-90°$C), δ 64.4 ppm (AuPPh$_3$); ^{13}C-{^{1}H} ($-70°$C), δ 200.8 (CO), 134.3 (d, C^2(Ph), J(PC) 15 Hz), 132.2 (d, C^1(Ph), J(PC) 46 Hz), 131.2 (C^4(Ph)), 129.2 ppm (d, C^3(Ph), J(PC) 12 Hz).

(vi) Compound VI, m.p. 210–213°C decomp., (Found: C, 42.2; H, 2.7. C$_{62}$H$_{45}$Au$_2$O$_8$P$_3$Ru$_3$S · $\frac{1}{2}$CH$_2$Cl$_2$ calcd.: C, 42.1; H, 2.6%). IR, ν(CO) in CH$_2$Cl$_2$, 2039s, 2008vs, 1975s, 1950s(br), 1913(sh) cm^{-1}. NMR, ^{1}H, δ 7.30 (m br, Ph); ^{31}P-{^{1}H} (CD$_2$Cl$_2$/CH$_2$Cl$_2$, at $-90°$C), δ 65.0 (d, AuPPh$_3$, J(PP) 18 Hz), 45.6 ppm (t, RuPPh$_3$, J(PP) 18 Hz); ^{13}C-{^{1}H}, δ 207.1 (br, 2 × CO), 202.5 (6 × CO), 137.2 (d, C^1(RuPPh), J(PC) 42 Hz), 134.4 (d, C^2(AuPPh), J(PC) 15 Hz), 134.2 (d, C^2(RuPPh), J(PC) 10 Hz), 132.9 (d, C^1(AuPPh), J(PC) 44 Hz), 130.9 (C^4(AuPPh)), 129.9 (C^4(RuPPh)), 129.0 (d, C^3(AuPPh), J(PC) 12 Hz), 128.2 ppm (d, C^3(RuPPh), J(PC) 10 Hz).

Reaction of PPh$_3$ with [Ru$_3$(μ-H)$_2$(μ_2-S)(CO)$_9$]

To a light petroleum (100 cm^3) solution of [Ru$_3$(μ-H)$_2$(μ_3-S)(CO)$_9$] (0.20 g, 0.34 mmol) was added powdered PPh$_3$ (0.12 g, 0.46 mmol), and the mixture was stirred for 2 h. After removal of solvent in vacuo, the crude mixture was dissolved in dichloromethane/light petroleum (1/5) and chromatographed on an alumina column (15 × 2 cm). Elution with dichloromethane/light petroleum (1/5) gave three bands identified as (a) unreacted [Ru$_3$(μ-H)$_2$(μ_3-S)(CO)$_9$], (b) yellow microcrystals of complex II (0.13 g, 47%), and (c) yellow microcrystals of IV (0.12 g, 33%). The IR and ^{31}P-{^{1}H} spectra of II and IV were identical with those of these species isolated from the reaction of [AuMe(PPh$_3$)] and [Ru$_3$(μ-H)$_2$(μ_3-S)(CO)$_9$] described above.

X-Ray diffraction studies

(a) Crystal structure of [Au$_2$Ru$_3$(μ_3-S)(CO)$_8$(PPh$_3$)$_3$] · 0.5 CH$_2$Cl$_2$ (VI)

Crystals of VI as its hemi-dichloromethane solvate were grown as dark red plates from dichloromethane/light petroleum. A crystal of approximate dimensions 0.4 ×

TABLE 3

ATOMIC POSITIONAL PARAMETERS (FRACTIONAL COORDINATES) ($\times 10^4$) AND ISO-TROPIC THERMAL PARAMETERS ($\text{Å}^2 \times 10^3$) WITH ESTIMATED STANDARD DEVIATIONS IN PARENTHESES FOR $[Au_2Ru_3(\mu_3\text{-S})(CO)_8(PPh_3)_3] \cdot \frac{1}{2}CH_2Cl_2$ (VI)

	x	y	z	U^a
Au(1)	2729(1)	1047(1)	1983(1)	35(1)
Au(2)	2946(1)	−88(1)	947(1)	35(1)
Ru(1)	2251(1)	−747(1)	1848(1)	31(1)
Ru(2)	3801(1)	−313(1)	2139(1)	38(1)
Ru(3)	2989(1)	−146(1)	3062(1)	41(1)
P(1)	2282(1)	2499(2)	1786(1)	35(1)
P(2)	2997(2)	347(2)	−56(1)	37(1)
P(3)	2023(1)	−2122(2)	1285(1)	36(1)
S(1)	3178(2)	−1484(2)	2529(1)	45(1)
O(1)	1017(5)	−881(5)	2460(4)	84(4)
O(2)	1195(4)	412(5)	960(4)	57(3)
O(3)	1994(7)	−874(8)	3828(5)	139(7)
O(4)	2750(5)	1812(6)	3427(4)	83(4)
O(5)	4167(7)	−287(8)	4202(4)	124(6)
O(6)	4465(5)	1491(6)	1892(5)	94(5)
O(7)	5024(5)	−605(9)	3211(4)	110(5)
O(8)	4521(5)	−1255(9)	1219(5)	125(5)
C(1)	1520(6)	−857(7)	2259(5)	50(4)
C(2)	1633(6)	−2(6)	1285(5)	48(4)
C(3)	2338(8)	−583(9)	3512(5)	79(6)
C(4)	2835(6)	1098(8)	3241(5)	49(4)
C(5)	3733(8)	−233(9)	3771(5)	74(6)
C(6)	4162(6)	835(7)	1968(5)	53(4)
C(7)	4563(6)	−497(9)	2811(5)	66(5)
C(8)	4194(5)	−923(9)	1526(6)	67(5)
C(111)	2149(5)	2964(6)	1002(4)	40(4)
C(112)	1745(7)	2472(8)	520(5)	60(5)
C(113)	1627(9)	2810(10)	−88(6)	86(7)
C(114)	1928(10)	3596(11)	−227(6)	98(8)
C(115)	2318(9)	4104(10)	253(7)	97(7)
C(116)	2438(7)	3795(8)	869(6)	68(5)
C(121)	2790(5)	3371(6)	2262(4)	39(4)
C(122)	3509(6)	3211(8)	2449(6)	63(5)
C(123)	3937(7)	3875(10)	2761(6)	76(6)
C(124)	3679(7)	4689(9)	2906(6)	66(5)
C(125)	2980(8)	4827(7)	2753(5)	63(5)
C(126)	2538(6)	4185(7)	2421(5)	48(4)
C(131)	1398(5)	2561(6)	1954(5)	37(3)
C(132)	948(5)	3263(6)	1740(5)	41(4)
C(133)	302(6)	3300(7)	1912(5)	52(4)
C(134)	114(6)	2621(8)	2258(6)	62(5)
C(135)	547(7)	1903(8)	2444(6)	63(5)
C(136)	1198(6)	1866(7)	2302(5)	50(4)
C(211)	3507(5)	1370(6)	−76(4)	39(4)
C(212)	3828(6)	1583(7)	−566(5)	54(4)
C(213)	4216(7)	2409(9)	−537(6)	67(5)
C(214)	4265(7)	2969(8)	−61(7)	71(6)
C(215)	3956(7)	2761(8)	432(6)	68(5)
C(216)	3578(6)	1971(7)	433(6)	57(5)

TABLE 3 (continued)

	x	y	z	U^a
C(221)	3411(6)	−519(6)	−463(4)	39(4)
C(222)	3015(6)	−1154(6)	−845(5)	49(4)
C(223)	3312(8)	−1836(8)	−1144(5)	61(5)
C(224)	4032(8)	−1874(8)	−1042(5)	65(6)
C(225)	4429(7)	−1271(8)	−646(6)	68(5)
C(226)	4118(6)	−600(7)	−352(5)	52(4)
C(231)	2167(6)	568(6)	−581(4)	42(4)
C(232)	2100(7)	1139(8)	−1083(5)	55(4)
C(233)	1447(7)	1286(8)	−1472(5)	63(5)
C(234)	866(7)	861(8)	−1356(5)	64(5)
C(235)	922(7)	277(8)	−849(6)	62(5)
C(236)	1566(6)	141(7)	−467(5)	54(4)
C(311)	2758(5)	−2762(6)	1108(4)	38(3)
C(312)	2988(7)	−3554(7)	1424(6)	64(5)
C(313)	3560(7)	−4030(8)	1298(7)	80(6)
C(134)	3873(7)	−3713(9)	835(7)	80(6)
C(315)	3651(7)	−2928(8)	520(6)	72(6)
C(316)	3114(6)	−2434(7)	663(5)	54(4)
C(321)	1381(5)	−2064(6)	545(4)	40(4)
C(322)	751(6)	−1644(7)	537(5)	54(4)
C(323)	226(7)	−1594(8)	7(6)	65(5)
C(324)	336(7)	−1959(8)	−536(6)	76(6)
C(325)	973(8)	−2378(8)	−549(6)	75(6)
C(326)	1482(7)	−2445(8)	−4(5)	62(5)
C(331)	1609(5)	−2983(6)	1703(5)	41(4)
C(332)	1749(6)	−3033(7)	2341(5)	49(4)
C(333)	1429(6)	−3681(7)	2640(6)	59(5)
C(334)	980(7)	−4292(7)	2311(6)	65(5)
C(335)	826(7)	−4251(8)	1679(7)	78(6)
C(336)	1140(7)	−3601(7)	1362(6)	63(5)
Cl(1)	517(6)	−275(7)	4679(5)	308(8)
C(9)	−324(21)	−527(24)	4906(16)	104(10)

^{a} Equivalent isotropic U defined as one third of the trace of the orthogonalised U_{ij} tensor.

0.4 × 0.075 mm was sealed in a thin-walled glass capillary under nitrogen for data collection.

Crystal data. $C_{62.5}H_{46}Au_2ClO_8P_3Ru_3S$, $M = 1782.6$, monoclinic, space group $P2_1/c$ (No. 14), a 19.577(12), b 14.645(11), c 21.901(8) Å, β 102.15(4)°, U 6138(6) Å^3, $Z = 4$, D_c 1.83 g cm^{-3}, $F(000) = 3395$, Mo-K_α X-radiation, graphite monochromator, $\overline{\lambda}$ 0.71069 Å, μ(Mo-K_α) 55.7 cm^{-1}.

Intensity measurements were recorded for a unique quadrant of reciprocal space in the range $3 \leqslant 2\theta \leqslant 50°$, using a Nicolet P3m diffractometer. Data were corrected for absorption by a Gaussian quadrature technique, maximum and minimum transmission factors being 0.655 and 0.129, respectively. Of a total of 7966 unique intensity data, remaining after deletion of systematic absenses and averaging of multiple and symmetry related measurements, 7082 with $I \geqslant 1.5\sigma(I)$ were used in structure solution and refinement. The structure was solved by the heavy atom method, and all non-hydrogen atoms, including those of the disordered solvent molecule, were located on difference Fourier syntheses. All these atoms were

TABLE 4

ATOMIC POSITIONAL PARAMETERS (FRACTIONAL COORDINATES) ($\times 10^4$) AND ISO-TROPIC THERMAL PARAMETERS ($\text{Å}^2 \times 10^3$) WITH ESTIMATED STANDARD DEVIATIONS IN PARENTHESES FOR $[Au_2Ru_3(\mu\text{-H})(\mu_3\text{-COMe})(CO)_9(PPh_3)_2]$ (VII)

	x	y	z	U^a
Au(1)	5840(1)	1395(1)	2677(1)	38(1)
Au(2)	7464(1)	3057(1)	2223(1)	37(1)
Ru(1)	6254(1)	4391(1)	2789(1)	35(1)
Ru(2)	4743(1)	2842(1)	3096(1)	34(1)
Ru(3)	5202(1)	2437(1)	1319(1)	29(1)
P(1)	6310(3)	−56(2)	3038(2)	38(1)
P(2)	9350(3)	3212(2)	2502(3)	42(1)
O(1)	5694(11)	6202(8)	3867(8)	84(6)
O(2)	6739(12)	5484(9)	1376(9)	96(7)
O(3)	8728(9)	5027(8)	4277(8)	78(5)
O(4)	2547(10)	1130(8)	2155(8)	79(5)
O(5)	5644(11)	2156(9)	4945(7)	88(7)
O(6)	3695(11)	4369(8)	4027(9)	87(6)
O(7)	2816(8)	1118(8)	105(7)	64(4)
O(8)	5304(11)	3316(8)	−330(7)	79(6)
O(9)	6166(8)	712(7)	519(6)	55(4)
O(10)	3641(7)	3872(6)	1619(6)	47(4)
C(1)	5911(12)	5532(9)	3447(9)	50(6)
C(2)	6558(12)	5072(10)	1909(11)	53(6)
C(3)	7843(11)	4739(9)	3657(10)	50(6)
C(4)	3348(13)	1759(12)	2478(11)	57(7)
C(5)	5339(12)	2354(10)	4237(9)	51(6)
C(6)	4075(13)	3796(11)	3675(10)	57(6)
C(7)	3700(11)	1605(9)	578(8)	39(5)
C(8)	5300(12)	3020(9)	319(9)	48(6)
C(9)	5903(11)	1363(8)	927(8)	39(5)
C(10)	4585(10)	3558(8)	2010(8)	35(5)
C(11)	3649(15)	4459(13)	955(12)	77(9)
C(112)	4905(7)	−1891(7)	3012(6)	62(7)
C(113)	3907	−2675	2612	65(7)
C(114)	3037	−2665	1786	79(9)
C(115)	3164	−1870	1362	83(9)
C(116)	4162	−1086	1763	56(7)
C(111)	5032	−1096	2588	41(5)
C(122)	8136(7)	268(8)	4759(6)	62(7)
C(123)	8653	444	5763	82(8)
C(124)	8006	434	6340	70(7)
C(125)	6841	248	5913	77(9)
C(126)	6323	72	4910	79(9)
C(121)	6971	83	4333	39(5)
C(132)	7193(6)	−1628(5)	2308(6)	57(6)
C(133)	8012	−1993	2035	63(7)
C(134)	8907	−1307	1990	62(7)
C(135)	8983	−256	2220	46(5)
C(136)	8164	108	2493	40(5)
C(131)	7268	−578	2538	41(5)
C(212)	8956(6)	1578(6)	922(6)	53(6)
C(213)	9191	1010	166	64(7)
C(214)	10151	1400	−6	72(9)

TABLE 4 (continued)

	x	y	z	U^a
C(215)	10875	2357	580	75(9)
C(216)	10640	2925	1336	75(9)
C(211)	9680	2535	1507	50(6)
C(222)	9677(7)	2801(8)	4261(7)	64(7)
C(223)	10249	2526	5081	85(9)
C(224)	11245	2242	5163	90(9)
C(225)	11670	2235	4425	94(1)
C(226)	11098	2510	3604	76(9)
C(221)	10102	2793	3522	47(5)
C(232)	9603(9)	5064(9)	2113(8)	81(9)
C(233)	10139	6090	2274	141(19)
C(234)	11151	6569	3063	155(22)
C(235)	11627	6023	3691	138(16)
C(236)	11091	4998	3530	84(9)
C(231)	10079	4518	2741	53(6)

^{a} Equivalent isotropic U defined as one third of the trace of the orthogonalised U_{ij} tensor.

assigned anisotropic thermal parameters and refined without constraint. Hydrogen atoms were restricted to idealised geometries (C–H, 0.96 Å) and isotropic thermal parameters fixed at ca. 1.2 times that of the carbon atoms to which they were attached. Blocked-cascade full matrix least squares converged to R 0.043 (R' 0.041).

(b) Crystal structure of [Au$_2$Ru$_3$(μ-H)(μ$_3$-COMe)(CO)$_9$(PPh$_3$)$_2$] (VII)

Orange prismatic crystals of VII [3] were grown from a dichloromethane/light petroleum solution. A crystal of approximate dimensions $0.6 \times 0.3 \times 0.3$ mm was chosen for data collection following the same procedures as above, with the exception that a full hemisphere of reciprocal space was scanned.

Crystal data. C$_{47}$H$_{34}$Au$_2$O$_{10}$P$_2$Ru$_3$, $M = 1517.0$ triclinic, space group $P\bar{1}$ (No. 2), a 13.016(4), b 13.803(4), c 15.124(4) Å, α 102.26(2), β 108.73(2), γ 100.15(2)°, U 2425(1) Å^3, $Z = 2$, D_c 2.07 g cm^{-3}, $F(000) = 1432$, Mo-K_α X-radiation, graphite monochromator, $\bar{\lambda}$ 0.71069 Å, μ(Mo-K_α) 70.3 cm^{-1}.

An empirical absorption correction was applied to the data, maximum and minimum transmission coefficients being 0.384 and 0.106, respectively. Of 9079 unique data, 6336 having $I \geqslant 2.5\sigma(I)$ were used in subsequent calculations. Structure solution and refinement proceeded as for VI above, with the exception that phenyl carbon atom positions were constrained (C–C 1.395 Å; C–C–C 120°). The hydrido ligand was also fixed (Ru–H, 1.85 Å) and methyl hydrogens constrained to tetrahedral geometry (C–H, 0.96 Å). As with VI, all hydrogen thermal parameters were fixed. Final residual indices were R 0.053 (R' 0.054).

For both structure determinations final difference electron density maps showed no peaks of chemical significance, the largest features being in the region of the metal atoms. The weighting scheme employed in the refinements was $w = [\sigma^2(F_0) + g|F_0|^2]^{-1}$ where $g = 0.0005$ for VI and $g = 0.0015$ for VII. All calculations were carried out on the Nicolet R3m/E structure determination system using programs of the SHELXTL system. Complex neutral atom scattering factors [17] were used throughout. Tables 3 and 4 list final atomic parameters for the non-hydrogen atoms.

Full listings of observed and calculated structure factors are available on request from the authors.

Acknowledgements

References

1 L.J. Farrugia, J.A.K. Howard, P. Mitrprachachon, J.L. Spencer, F.G.A. Stone and P. Woodward, J. Chem. Soc., Chem. Commun., (1978) 260.
2 B.F.G. Johnson, D.A. Kaner, J. Lewis, P.R. Raithby and M.J. Taylor, J. Chem. Soc., Chem. Commun., (1982) 314; idem, Polyhedron, 1 (1982) 105; B.F.G. Johnson, D.A. Kaner, J. Lewis and P.R. Raithby, J. Organomet. Chem., 215 (1981) C33.
3 M. Green, K.A. Mead, R.M. Mills, I.D. Salter, F.G.A. Stone and P. Woodward, J. Chem. Soc., Chem. Commun., (1982) 51; L.W. Bateman, M. Green, J.A.K. Howard, K.A. Mead, R.M. Mills, I.D. Salter, F.G.A. Stone and P. Woodward, ibid., (1982) 773.
4 J.W. Lauher and K. Wald, J. Am. Chem. Soc., 103 (1981) 7648.
5 M.I. Bruce and B.K. Nicholson, J. Chem. Soc., Chem. Commun., (1982) 1141.
6 P. Braunstein, G. Predieri, A. Tiripicchio and E. Sappa, Inorg. Chim. Acta, 63 (1982) 113.
7 R.D. Adams and D.A. Katahira, Organometallics, 1 (1982) 53.
8 K. Wade, Adv. Inorg. Chem. Radiochem., 18 (1976) 1; in B.F.G. Johnson (Ed.), Transition Metal Clusters, Wiley, New York, 1980, Ch. 3.
9 W.B. Pearson, Lattice Spacings and Structures of Metals and Alloys, Pergamon Press, London, 1951.
10 D.M.P. Mingos, J. Chem. Soc., Dalton Trans., (1976) 1163.
11 M.J. Mays, P.R. Raithby, P.L. Taylor and K. Hendrick, J. Organomet. Chem., 224 (1982) C45.
12 G.M. Sheldrick and J.P. Yesinowski, J. Chem. Soc., Dalton Trans., (1975) 873.
13 A.G. Orpen, J. Chem. Soc., Dalton Trans., (1980) 2509.
14 D.M.P. Mingos, Nature (Phys. Sci.), 236 (1972) 99.
15 J.W. Lauher, J. Am. Chem. Soc., 100 (1978) 5305.
16 K.P. Hall, B.R.C. Theobald, D.I. Gilmour, D.M.P. Mingos and A.J. Welch, J. Chem. Soc., Chem. Commun., (1982) 528.
17 International Tables for X-Ray Crystallography, Kynoch Press, Birmingham, 1974, Vol. 4.